Methionine Radical Cation: Structural Studies as a Function of pH Using X- and Q-Band Time-Resolved Electron Paramagnetic Resonance Spectroscopy

Haruhiko Yashiro,[†] Ryan C. White,[†] Alexandra V. Yurkovskaya,*[,‡] and Malcolm D. E. Forbes*[,†]

Venable and Kenan Laboratories, Department of Chemistry, CB#3290, University of North Carolina, Chapel Hill, North Carolina 27599, and International Tomography Center, Institutskaya 3a, 630090 Novosibirsk, Russia

Received: March 25, 2005; In Final Form: April 12, 2005

A comprehensive high resolution electron paramagnetic resonance (EPR) characterization of the L-methionine radical cation and its *N*-acetyl derivative in liquid solution at room temperature is presented. The cations were generated photochemically in high yield by excimer laser excitation of a water soluble dye, anthraquinone sulfonate sodium salt, the excited triplet state of which is quenched by electron transfer from the side chain sulfur atom of methionine or *N*-acetylmethionine. The radicals were detected by continuous wave (CW) time-resolved electron paramagnetic resonance (TREPR) spectroscopy at X-band (9.5 GHz) and Q-band (35 GHz) microwave frequencies. At pH values well below the pK_a of the protonated amine nitrogen, the cation forms a dimer with another ground-state methionine molecule through a S−S three-electron bond. In basic solution, the lone pair on the nitrogen of the amino acid is available to make an intramolecular S−N three-electron bond with the side chain sulfur atom, leading to a five-membered ring structure for the cation. When the amino acid nitrogen is unsubstituted (methionine itself), rapid deprotonation to an aminyl radical takes place at high pH values. If the nitrogen is substituted (*N*-acetylmethionine), the cyclic structure is observed within its electron spin relaxation time at about 1 μs. Spectral simulation provides chemical shifts (*g*-factors) and hyperfine coupling constants for all structures, and isotopic labeling experiments strongly support the assignments.

Introduction

Amino acid side chain redox chemistry and free radical chemistry are critical parts of many biological reaction mechanisms,[1] and a detailed characterization of the reactive intermediates involved is highly desirable. The process of oxidation at sulfur in methionine (Chart 1, top right) to give a radical cation (**1**) has been implicated in several important biochemical reaction pathways, notably glycation of proteins and subsequent disease development such as glaucoma.[2] The redox chemistry of methionine within proteins is currently a topic of great interest. Much of this attention stems from the fact that the oxidation of methionine has been directly linked to amyloid fibril formation in neurological biochemistry. This process is suspected to be the first in a cascade of many chemical reactions leading to symptoms of Alzheimer's disease.[3]

The methionine radical cation is therefore a paramagnetic reactive intermediate of great importance, whose structure and reactivity need to be clearly understood. The cation itself and several model systems have been investigated indirectly by several different physical methods in solution, and in glassy matrixes or single crystals by electron paramagnetic resonance (EPR) spectroscopy. However, high resolution EPR characterization of **1** or its *N*-acetyl derivative (**2**, Chart 1, bottom left) in aqueous solution has not been reported to date. Our research

CHART 1

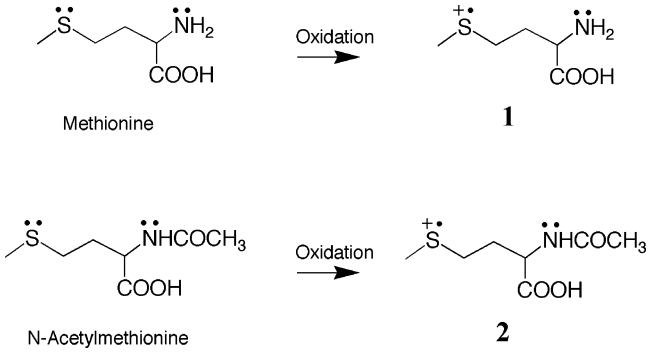

groups have had a long-standing interest in the redox chemistry of amino acids[4] and short peptides,[5] and in this paper, we turn our attention to the radical chemistry of methionine as a function of pH at room temperature.

Scheme 1 shows the spectrum of reactivity that has been proposed in the literature during the past 30 years for cation **1** and various structural analogues. The first magnetic resonance spectra of such cations were recorded by Kominami[6] and Kawatsura et al.,[7] who reported EPR parameters from γ-irradiated single crystals of DL-methionine. Along with Naito et al.'s EPR work on ^{33}S substituted methionine in 1977,[8] these early papers clearly established that oxidation occurs preferentially at sulfur. Later, pulse radiolysis experiments by Asmus et al.,[9] along with further work by Naito and co-workers,[10] provided evidence for dimeric structures such as **5a** containing S−S three-

* To whom correspondence should be addressed. E-mail: mdef@unc.edu (M.D.E.F.); yurk@tomo.nsc.ru (A.V.Y.).
[†] University of North Carolina.
[‡] International Tomography Center.

10.1021/jp051551k CCC: $30.25
Published on Web 06/08/2005

SCHEME 1

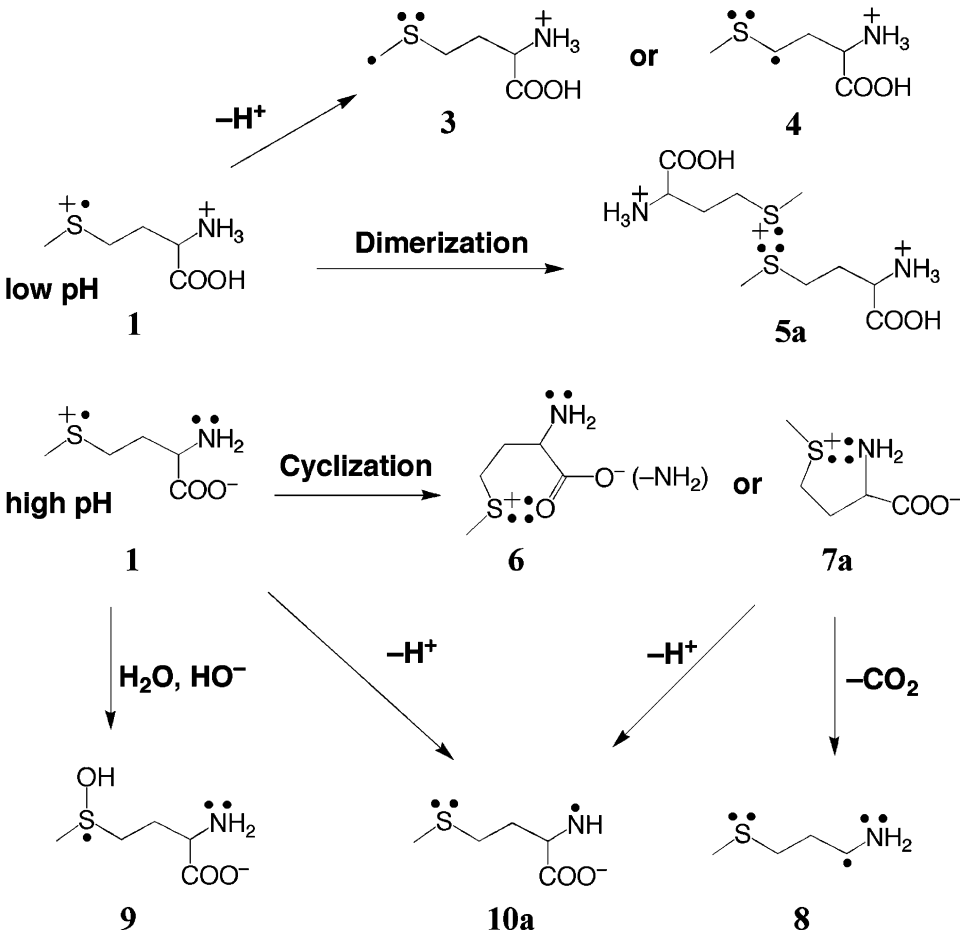

electron bonds as well as neighboring group effects with heteroatoms such as nitrogen and oxygen. Such neighboring group effects led these researchers to postulate six- and five-membered ring intermediate structures with S−O and S−N three-electron bonds (e.g., **6** and **7a** in Scheme 1), whose formation was dependent on the pH of the solution. Bobrowski and co-workers have conducted extensive studies of the oxidation chemistry of methionine and have proposed similar cyclic structures[11] as well as the possibility that the hydroxyl radical, at pH > 10, can assist in decarboxylation of the radical cation in certain short peptide sequences.[12] In the case of a single methionine molecule, the decarboxylation reaction would lead to α-amino (or α-amido) radicals such as **8**. There is also some evidence for the existence of hydroxy sulfuranyl radicals (e.g., **9**) in the solution chemistry of this amino acid.[13] The majority of the early literature reports on this topic have provided evidence for the dimeric S−S bonded structure **5a** at pH < 7 and the five-membered ring S−N bonded structure **7a** at pH > 10. (To simplify the notation, throughout this paper, we will refer to intermediates produced specifically from methionine with the letter a in the compound number and those from *N*-acetylmethionine with the letter b).

The low temperature steady-state EPR experiments of Champagne et al. showed that the cyclic structure **7a** is formed in the solid state.[14] Their data lacked the resolution available in liquid solution experiments, and for this reason, their *g*-factor measurements were reported to only three significant figures. Resonance Raman experiments on (3-(methylthio)propylamine), a model compound for **1**, by Tripathi and Tobien[15] also supported the existence of the five-membered ring structure, and they suggested that it forms through an −SOH type intermediate such as **9**. Recent papers by Schoeneich and co-workers have suggested that the six-membered ring structure **6** with an S−O three-electron bond is an important intermediate with regard to the *β*-amyloid fibril formation reaction.[16] It should be noted that the suggested presence of structure **6** is limited to cases where the methionine residue is part of a protein or short peptide, and not a free-standing amino acid. They have also reported evidence for the existence of **6** in product analysis studies using the hydroxyl radical as the oxidant.[17] However, those experiments were carried out with the amide of methionine, and not the amino acid itself (this is why we have shown an amide group in parentheses for structure **6** in Scheme 1). There may be subtle steric or electronic factors that favor a S−O bond over a S−N bond in some derivatives of methionine. New ab initio calculations by both the Schoeneich group[18] and Huang and Rauk[19] support this. The latter paper also suggests that the deprotonation reaction of the noncyclic structure to give α-thio alkyl radicals (**3** or **4**) may also be a possible reaction pathway. In this regard, deprotonation of the five-membered ring structure to give the linear aminyl radical **10a** may also be important.

In other experiments using magnetic resonance detection, there have been several reports offering indirect evidence for some of the structures shown in Scheme 1. An interesting study of this chemistry was reported by Goez et al.,[20] who used steady-state chemically induced dynamic nuclear polarization (CIDNP) measurements of products formed from the S−N bonded five-membered ring structure. They discussed their results in terms

CHART 2

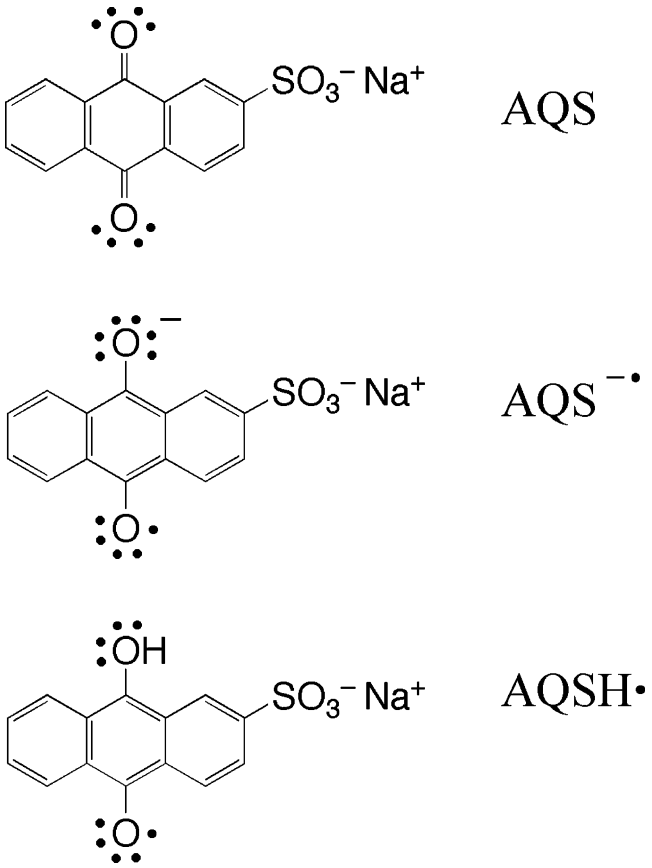

of a dynamic equilibrium between the linear and cyclic species and concluded that formation of the cyclic cation was "not strongly exergonic".[21] A study by Korchak et al.[22] reported the magnetic field dependence of the CIDNP signals, which led to estimates of some of the hyperfine interactions in the cyclic structure; we will comment further on those results in the discussion section below. These CIDNP experiments represent the only high resolution magnetic resonance characterization of methionine-related redox intermediates to date, yet still a precise map of the spin density distribution in cations **5a** and **7a** has remained elusive.

Several of the reactions described in Scheme 1 may be fast at room temperature, and therefore, the concentration of **1**(**2**), **5a**(**b**), or **7a**(**b**) in such solutions may be too low to detect by conventional steady-state EPR methods. This is to be expected especially for the decarboxylation and deprotonation reactions. We have circumvented this problem in two ways. First, by using the time-resolved EPR (TREPR) method, we detect the cation when there are large concentrations of it present, before any secondary reactions can take place. Second, when the amide nitrogen is acetylated, the secondary reactions are retarded to such an extent that the lifetime of the cyclic structure in solution may be extended significantly. Below, EPR data on the redox chemistry of methionine will be presented and discussed. We will also present results from *N*-acetylmethionine, which is a good model compound for Met-containing proteins because of the amide bond at the N-terminus.

In this work, we use anthraquinone sulfonate sodium salt (AQS, Chart 2, top) as a photosensitizer for the production of cations **1** and **2** in high yield in aqueous solutions over a wide pH range. Excitation of AQS at 308 nm (XeCl excimer laser) leads cleanly and quickly to a triplet excited state (^{3}AQS*) which is quenched by good electron donors. The energetically low-lying electron on the sulfur of the methionine side chain is quickly transferred to ^{3}AQS*, leading to high concentrations ($\sim 10^{-5}$ M) of the methionine radical cation and the AQS radical anion ($AQS^{-\bullet}$, Chart 2, center) in less than 100 ns in aqueous solution. AQS is an excellent sensitizer for this chemistry, with a high extinction coefficient at 308 nm, a high quantum yield for formation of the triplet, and a triplet state that is an excellent electron acceptor.[23] It also produces intense triplet mechanism spin polarization[24] in the intersystem crossing process, which leads to good signal-to-noise ratios in our experiment. An additional advantage of this sensitizer is that the radical anion $AQS^{-\bullet}$ (Chart 2, middle) has very small hyperfine couplings and in almost all of our experiments appears as a single sharp line. Therefore, it does not interfere or overlap very much with other radicals' EPR signals.

In low pH solutions, the $AQS^{-\bullet}$ radical anion is expected to be protonated rapidly to form the $AQSH^{\bullet}$ radical (Chart 2, bottom). We base this on the fact that the pK_a of the conjugate acid of the closed shell anion is 3.9[25] and the assumption that the conjugate acid of the open shell radical ion should have approximately the same acid−base properties. The neutral $AQSH^{\bullet}$ radical is also strongly polarized by the triplet mechanism and has a very narrow spectral width, although it is broader than the $AQS^{-\bullet}$ signal due to a small hyperfine coupling to the extra H atom. For this reason, it appears as a narrow, sharp doublet in our experiments (at least at later delay times, vide infra), slightly upfield from $AQS^{-\bullet}$ due to a smaller *g*-factor.

Below, we will present high resolution TREPR spectra of cations and other radicals from reactions of methionine and *N*-acetylmethionine with photoexcited AQS. Characterization data in the form of electron chemical shifts (free radical *g*-factors) and isotropic hyperfine coupling constants will be put forward and discussed. With this particular system, it is advantageous to conduct the TREPR experiment at the Q-band microwave frequency (35 GHz), where chemical shift resolution is higher than the standard X-band spectrometer. Our experimental strategy is to use isotopic substitution to confirm hyperfine coupling constants and to use spectra acquired at two different frequencies to improve the precision of our *g*-factor measurements. In some cases, running the experiment at a higher frequency also leads to more accurate hyperfine coupling constants because it can eliminate the problem of spectral overlap that often plagues EPR analysis at lower frequencies. The details of the TREPR experiment are described elsewhere.[26]

Results and Discussion

Figure 1 shows X-band TREPR spectra obtained at room temperature in aqueous solution of pH 2 when AQS is irradiated in the presence of L-methionine. In Figure 1A, the spectrum obtained at a delay time of 700 ns after the laser flash is shown, with a simulation overlaid. The spectra exhibit strongly emissive transitions due to the triplet mechanism of chemically induced electron spin polarization (CIDEP),[24] a well understood phenomenon and typical for radicals or radical ions produced from excited states of quinones.[27] The simulation in Figure 1A uses two sets of hyperfine coupling constants resulting from interaction of the unpaired electron with six equivalent methyl protons and four equivalent methylene protons, respectively. Such a hyperfine coupling pattern can only arise from a dimer type structure such as **5a** in Scheme 1. The concentration dependence of this TREPR signal also supports this conclusion: The signal intensities are proportional to the square of the concentration; however, we were never able to go low enough in concentration

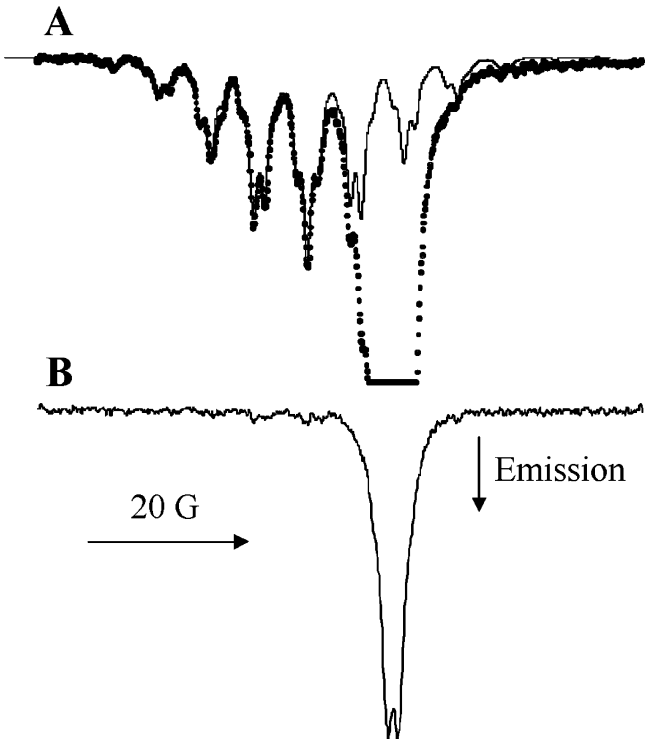

Figure 1. Time dependence of the X-band TREPR spectra taken upon irradiation of L-methionine and AQS in H_2O (pH 2.0) at (A) 0.7 μs (dotted line) and (B) 2.0 μs. Simulation (radical **5a**) of A is overlaid (solid line) on the experimental spectrum. The magnetic field sweep width is 80 G. The TREPR intensity (y axis) is in arbitrary units. In this and all subsequent spectra, lines below the baseline are in emission, while those above the baseline are in enhanced absorption.

to see the monomeric cation before going below the sensitivity of the apparatus. The g-factor and coupling constants used for the simulation are in good agreement with those found in model systems by other research groups.[28] The $AQS^{-\bullet}$ signal was simulated using a single broad line, as no hyperfine splittings were resolved at this delay time (small couplings in continuous wave (CW) TREPR spectroscopy are lifetime broadened significantly at delay times less than 1 μs).

Figure 1B shows the same system detected at 2 μs after the laser flash, where only the $AQSH^{\bullet}$ radical is observed (large emissive doublet). The disappearance of the signal from the methionine dimer radical cation on this time scale is most likely due to two processes: spin−lattice relaxation and degenerate electron exchange. It is reasonable to expect that the dimer will relax faster than the $AQSH^{\bullet}$ radical due to the heavy atom effect of the sulfurs. The exchange reaction, while not a chemical decay process in itself, will quench polarization due to scrambling of the nuclear spin systems.

Figure 2 shows the pH dependence of the methionine/AQS system as detected by TREPR 200 ns after flash photolysis at 308 nm. The resolution is not as good as that in Figure 1 due to the earlier delay time of detection. Clearly, there is an evolution of the dimer signal to a different carrier at about pH 9, which is at approximately the pK_a value of the protonated nitrogen of the amino group. The higher pH spectra are at first glance a bit confusing to decipher because of the intensities of the transitions, which do not appear to be all emissive (E) or absorptive (A), nor do they follow any familiar pattern of CIDEP such as low field E, high field A, which would be expected from the radical pair mechanism. We will comment further on the intensities below, but note here that there are not many transitions and they are well spaced, indicating that only a few

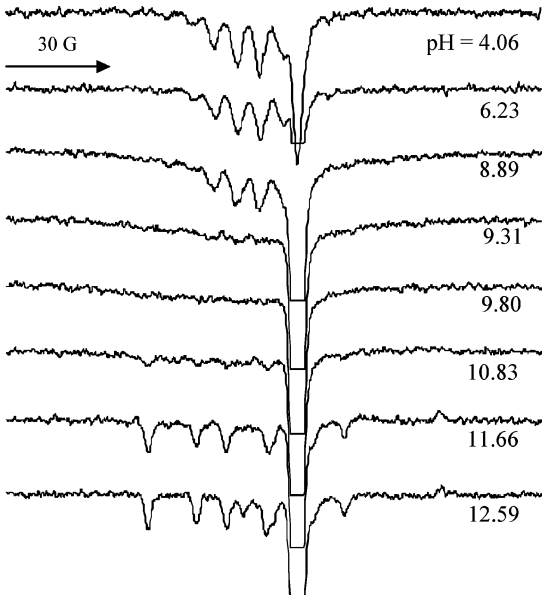

Figure 2. pH-dependent X-band TREPR spectra taken of L-methionine and irradiated AQS in H_2O at a 0.2 μs delay time. The pH values are shown directly below the spectra. The sweep width for all spectra is 150 G.

hyperfine coupling constants are present. This does not fit the expected pattern for the cyclic structure **7a**, which leads us to suggest either that the cyclic structure is not formed or that once formed it has another chemical decay pathway available to it such as deprotonation at nitrogen. Our simulations, presented and discussed below, support the latter hypothesis.

The spin polarization pattern observed in Figures 1 and 2 is dominated by the triplet mechanism, which is strongly emissive, as expected for photochemical reactions from quinone triplet states.[27] The $AQS^{-\bullet}$ radical formed in basic solution has a g-factor of 2.0040 and appears as a broad single line due to unresolved hyperfine interactions on the aromatic ring. In acid solution, the $AQSH^{\bullet}$ radical is observed due to rapid protonation at oxygen, and the signal appears as an emissive doublet with a g-factor of 2.0034, slightly upfield from $AQS^{-\bullet}$. We have expanded the spectra vertically to show the detailed hyperfine structure of the other radicals; therefore, the g-factor difference in the two AQS-based radicals is not visible. However, in our Q-band spectra reported below, it will be very obvious that there are two different counterradical signal carriers as a function of pH. The advantage of using AQS as a sensitizer is that it does not overlap much with the other radicals, allowing for their more precise characterization. It is a better choice for EPR studies than 4-carboxybenzophenone, for example, which has been used by other researchers for amino acid oxidation studies[22,29] but has multiple hyperfine interactions that overlap to a large extent with the other radicals' signals at $g = 2$.

Figure 3A shows the TREPR spectrum acquired at pH > 12 from Figure 2, along with a simulation in Figure 3B using literature parameters for a typical aminyl radical **10**.[30] At these pH values, deprotonation of the cyclic methionine radical cation to the aminyl radical **10a** is facile, and here, the y axis is expanded and the data signal averaged slightly longer to show all the TREPR transitions. Examination of Scheme 1 shows that there are two pathways by which the aminyl radical can be produced: loss of a proton from the cyclic structure **7a** or electron transfer from nitrogen to sulfur after the initial creation of the noncyclic cation **1**, followed by loss of a proton. In fact, there is a third pathway (not shown in the scheme) involving direct photooxidation of the nitrogen followed by proton loss,[29]

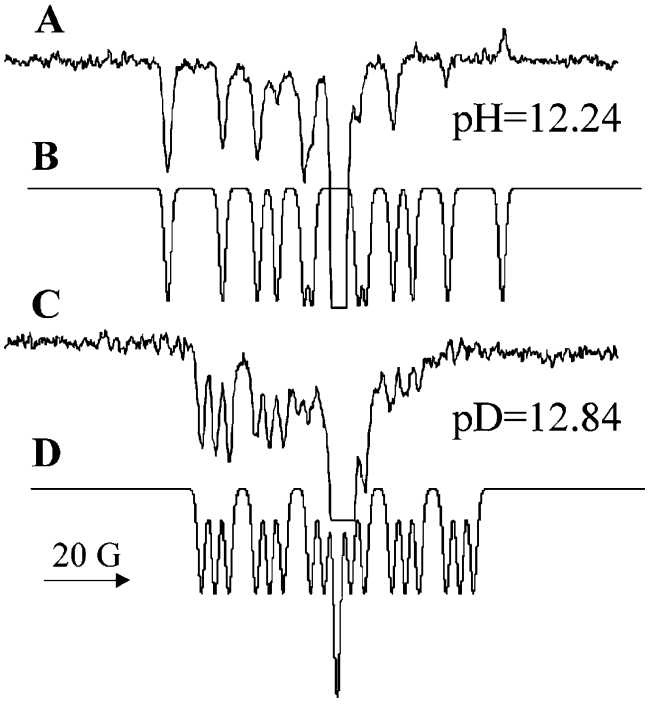

Figure 3. High pH/pD X-band TREPR spectra of L-methionine and irradiated AQS taken at a 0.2 μs delay time in (A) H_2O and (C) D_2O. Exact pH/pD values are shown below the corresponding spectra. (B and D) Simulations of A and C, respectively (radicals **10a** and **10a-N-d$_1$**). The sweep width for both experimental spectra is 150 G.

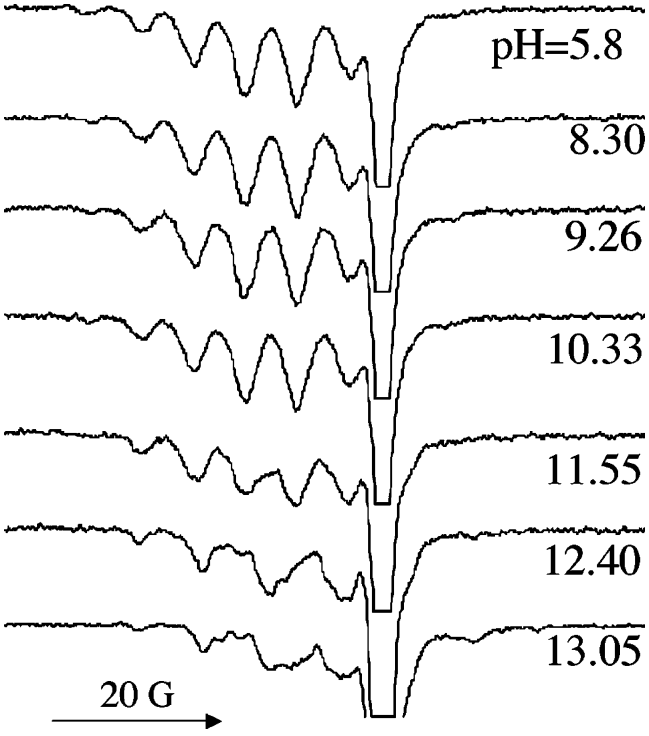

Figure 4. pH-dependent X-band TREPR spectra of *N*-acetyl L-methionine and irradiated AQS in H_2O at a 0.2 μs delay time. Exact pH values are shown directly below the spectra. The sweep width for all spectra is 80 G.

but we rule this out on the basis of the much lower ionization potential for the sulfur lone pair electrons. This difference in ionization potentials also leads us to rule out the second pathway described above, as it is unlikely that an uphill electron transfer event will occur on this time scale, especially with a flexible spacer between the donor and the acceptor. We conclude that the most likely pathway for production of the aminyl radical at room temperature from methionine above pH 9 is loss of a proton from the cyclic radical cation, which then no longer remains in the cyclic geometry because the stabilization of the positive charge on the sulfur atom is not necessary. In some of the broader spectra in Figure 2, at about pH 7 or 8, the cyclic structure may be present but significantly lifetime broadened by this process or by the cyclization process itself, which may be dynamic on this time scale. We will comment further on this possibility below.

It is important to note that the simulation in Figure 3B only attempts to reproduce line positions and chemical shift information and not the intensities. As noted above, the intensities of the transitions in Figure 3A are quite unusual, with some lines nearly being canceled out and others appearing in absorption where one would predict emission. We suggest that this pattern arises because of what is known as a spin "memory effect".[31] The initially formed cation contains two protons on the amine nitrogen, both of which are coupled to the unpaired electron. The radical pair mechanism spin polarization is created in the initial radical. Deprotonation takes place mostly after this polarization has formed, but the resulting aminyl radical has one less proton and therefore carries the splitting pattern of the second radical. However, each transition remembers the spin polarization obtained in the first radical. This is an interesting phenomenon in its own right which has been observed many times in solution phase CIDNP experiments[32] and in solid-state TREPR experiments on, for example, photosynthetic reaction centers.[33] However, to the best of our knowledge, the detection of a memory effect for noninteracting monoradicals in liquid solution by TREPR has not been reported previously. A model for this interesting reaction is currently being developed which will be reported in a future publication.

To further support the assignment of the spectrum in Figure 3A to the aminyl radical, the experiment was run in D_2O instead of H_2O. This is expected to result in efficient deuterium exchange at nitrogen, which should give radicals with different spectral patterns for either the cyclic structure or the aminyl radical. The resulting experimental TREPR spectrum is shown in Figure 3C along with a simulation (Figure 3D) that uses the same hyperfine coupling constants as those for the simulation in Figure 3B except that the aminyl proton now has $I = 1$ and a coupling constant of 6.5 less than its protonated analogue. It is interesting to note that the spectral intensities in Figure 3C follow the same deviation in intensities as the protonated analogue. This follows in a manner consistent with our model for sequential radicals and a memory effect discussed above. Again, it should be noted that no effort is made in these simulations to account for the deviations from "normal" CIDEP intensities; only the line positions have been used to make the structural assignment.

To better characterize the cyclic radical cation **7a**, it was recognized that the deprotonation reaction leading to the aminyl radical **10a** had to be slowed so that the cyclic structure could be observed directly by TREPR. To accomplish this, we used *N*-acetylmethionine (**2**), which changes the N-terminus of the amino acid from an amine to an amide. This increases the pK_a of the proton on the N-terminus by almost 15 units.[34] In this case, the cyclic structure, once formed, should have a much longer lifetime than that for methionine. Scheme 2 shows how acetylation simplifies the possible redox chemistry with AQS. Figure 4 shows the pH dependence of the X-band TREPR spectra acquired after irradiation of the *N*-acetylmethionine/AQS system. At low pH, an 11-line pattern is observed from 10 nearly

SCHEME 2

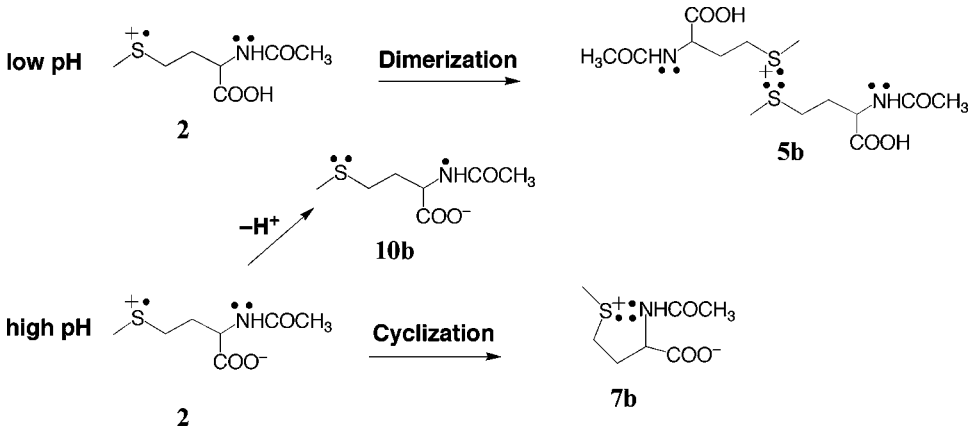

equivalent protons, as in Figure 1A; therefore, this signal is assigned to the dimer radical cation **5b**. Clearly, a new signal carrier grows in at high pH that is different from the dimer spectrum. Furthermore, this new signal is not due to the aminyl radical observed in Figures 2 and 3, as it has a completely different hyperfine pattern (cf. Figure 2, bottom, and Figure 3, top).

Figure 5A shows the pH 5.8 spectrum from Figure 4, next to a spectrum run in D_2O as the solvent instead of H_2O (Figure 5B). It is clear that there is no isotope effect upon deuterium substitution at the N-terminus of this derivative of the methionine radical cation. The simulation in Figure 5C reproduces both spectra extremely well, and we assign both spectra to the dimer **5b** of the radical cation of *N*-acetylmethionine. We will comment further on the absent isotope effect when the high pH data from Figure 4 are considered below. The parameters used in the simulation are listed in Table 1. The hyperfine coupling constants are slightly different than those for the methionine radical cation, decreasing for the methyl protons

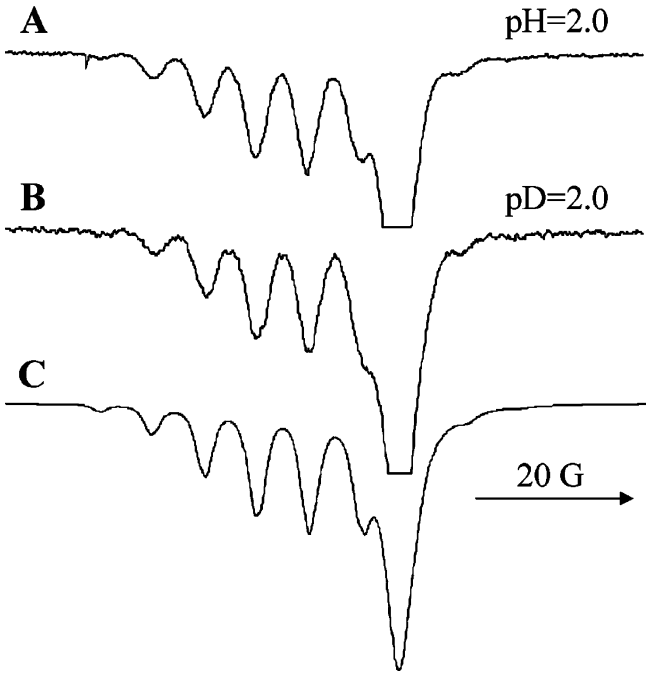

Figure 5. Low pH/pD X-band TREPR spectra of *N*-acetyl L-methionine and irradiated AQS taken at a 0.2 μs delay time in (A) H_2O and (B) D_2O. Exact pH/pD values are shown above the corresponding spectra. (C) Simulation of A (radical **5b**). The sweep width for both spectra and the simulation is 80 G.

TABLE 1: Radicals Characterized and Parameters Used for Simulation of TREPR Spectra

Radical Structure[a]	Hyperfine Coupling Constants (G)
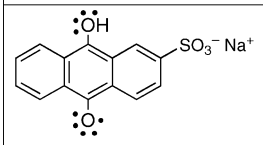 **AQSH·**	1.8 (O–H)
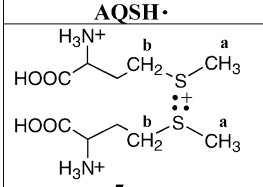 **5a**	7.12 ($6H_a$) 5.66 ($4H_b$)
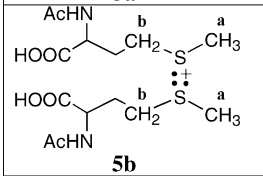 **5b**	6.92 ($6H_a$) 6.05 ($4H_b$)
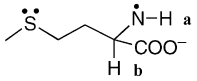 **10a**	13.36 (N) 21.92 (H_a) 33.30 (H_b)
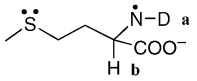 **10a–N–d_1**	13.36 (N) 3.32 (D_a) 33.30 (H_b)
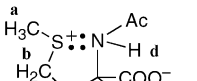 **7b**	8.30 ($3H_a$) 7.38 ($2H_b$) 1.35 (H_c) 9.57 (H_d) 0.10 (N)
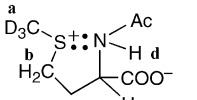 **7b–d_3**	1.27 ($3D_a$) 7.38 ($3H_b$) 1.35 (H_c) 9.57 (H_d) 0.10 (N)
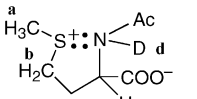 **7b–N–d_1**	8.30 ($3H_a$) 7.38 ($3H_b$) 1.35 (H_c) 1.47 (D) 0.10 (N)

[a] The *g*-factor and line width for $AQS^{-\bullet}$ were taken from ref 23. Other *g*-factors: $AQSH^{\bullet}$ = 2.00337, **5a** and **5b** = 2.01012, **10a** and **10a**−**N**−$\mathbf{d_1}$ = 2.00428, **7b**, **7b**−$\mathbf{d_3}$, and **7b**−**N**−$\mathbf{d_1}$ = 2.00729. Line widths varied from 1.02 to 1.23 G and were optimized for best fit along with the listed hyperfine coupling constants, which are all from this work.

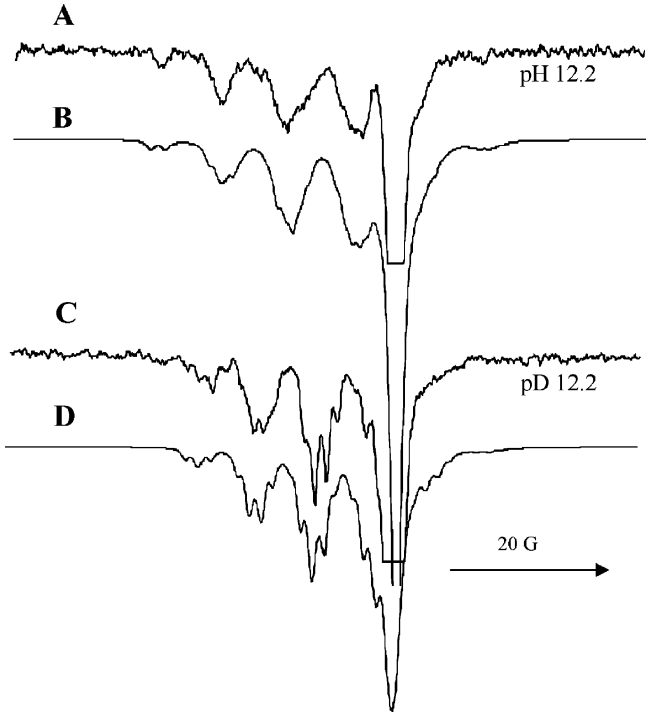

Figure 6. High pH/pD X-band TREPR spectra of irradiated *N*-acetyl L-methionine and AQS taken at a 0.2 μs delay time in (A) H_2O and (C) D_2O. Exact pH/pD values are shown directly below the spectra. (B and D) Simulations of A and C, respectively (radicals **7b** and **7b-N-d$_1$**). The sweep width for both spectra and simulations is 80 G.

CHART 3

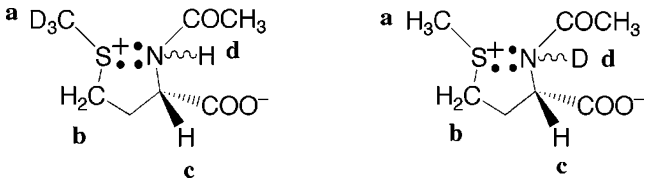

while increasing slightly for the methylene protons. This is an expected result, as the carbonyl moiety of the acetyl group is electron withdrawing and so the shift in electron density for this species is in the predicted direction.

Figure 6A shows the TREPR spectrum from Figure 4 acquired at pH 12.2. Immediately below it in Figure 6B is a simulation, using parameters listed in Table 1, that is consistent with the five-membered ring, S−N three-electron bonded, cyclic radical cation of *N*-acetylmethionine (**7b**). To provide further support for this assignment, we performed the two isotopic substitutions illustrated in Chart 3. The first substitution was carried out as before by running the experiment in D_2O, where we expect H/D exchange at the N-terminus (Chart 3, right-hand side). In this case, we expect to see little or no effect for the dimer structure at low pH because there are no exchangeable protons near the radical center in the dimer, and this is indeed the case as per our discussion of Figure 5 above; the spectra of the dimer in H_2O and D_2O are identical. At high pH, however, an isotope effect on the spectrum is observed (Figure 6C) and the simulation below the experimental spectrum (Figure 6D) tells us that the deuterium substitution was made at the amide nitrogen. The simulation was carried out once again with all parameters from the protonated structure in Figure 6A except for the deuterium atom on nitrogen which was given $I = 1$ and a coupling constant of 6.5 times less than that of the corresponding proton (Table 1).

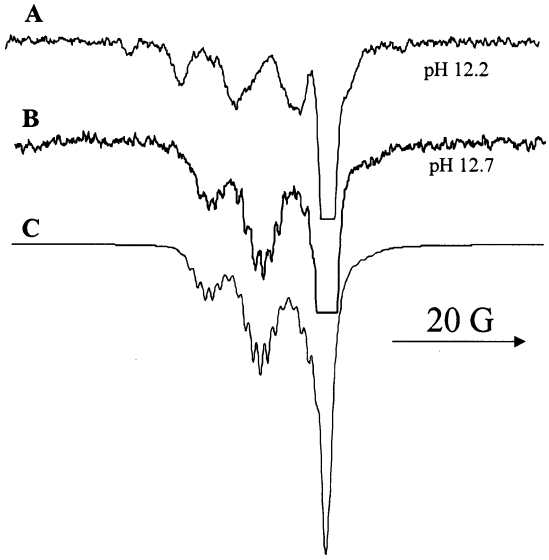

Figure 7. High pH X-band TREPR spectra of irradiated AQS and (A) *N*-acetyl L-methionine taken at a 0.2 μs delay time and (B) *N*-acetyl L-methionine-methyl-d_3 taken at 0.4 μs in H_2O. Exact pH values are shown below the spectra. (C) simulation of B (radical **7b-d$_3$**). The sweep width of both spectra is 80 G.

Additional support for the cyclic structure comes from isotopic substitution at the methyl group on the side chain of *N*-acetylmethionine (Chart 3, left-hand side). A sample of L-methionine with a CD_3 group in place of the CH_3 group was purchased and converted to the *N*-acetylmethionine-d_3. A subsequent TREPR experiment with ^{3}AQS* oxidation at high pH led to the spectrum shown in Figure 7B. The protonated analogue is shown for comparison immediately above it in Figure 7A. There is a large change in the spectral width and number of transitions between these two spectra. Once again, spectral simulation with the predictable changes in spin quantum number and coupling constant for those three protons/deuterons leads to excellent agreement (Figure 7C, Table 1) for the cyclic structure.

The coupling constants obtained for the cyclic cation of *N*-acetylmethionine are all hyperconjugative in nature except for the nitrogen. This is of interest because each coupling to these protons should be dependent on the dihedral angle and therefore to the ring conformations and/or dynamics. This will be commented on further below, but it should be noted herethat the proton coupling constants are all smaller than those usually observed for five-membered rings[35] and this may be due to the $\sigma-\sigma^*$ nature of the three-electron bond, vide infra. In such cases, the hyperfine interactions might be expected to fall between those of a neutral radical and, say, a radical anion where all coupling constants are typically much smaller than their neutral counterparts due to the distance of the unpaired electron from the nuclei. In some cases, this difference in hyperfine values can be an order of magnitude.

Figure 8 shows TREPR spectra of the *N*-acetylmethionine/AQS system measured at the Q-band microwave frequency. As mentioned above, deprotonation of this radical cation is slow even in strongly basic solution because it is an amide rather than an amine. Therefore, the dimer **5b** is observed at low pH and the cyclic structure **7b** at high pH. This experiment allowed very accurate *g*-factors to be obtained using field/frequency measurements and comparison to the X-band spectrum (Table 1). The observed splitting patterns are the same as those at the X-band for each radical and are almost completely separated from the AQS signals at the Q-band. It should be noted that in

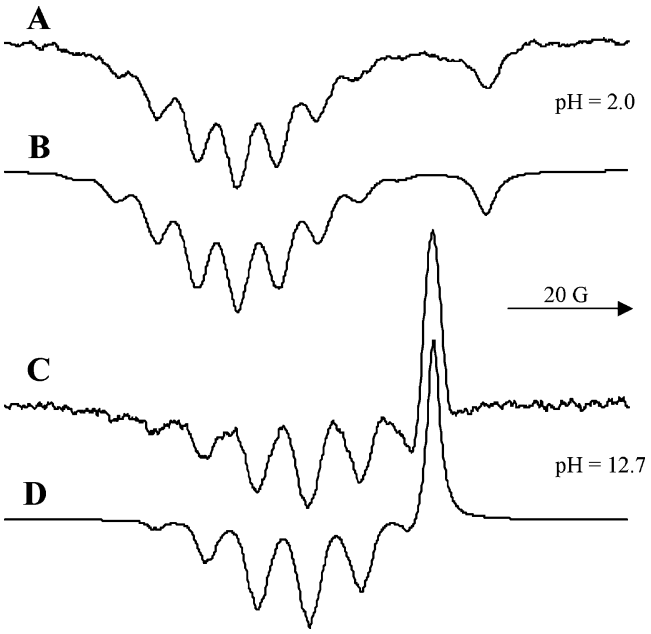

Figure 8. Q-band TREPR spectra of *N*-acetyl L-methionine and irradiated AQS in H_2O at (A) pH 2.0 taken at a 0.4 μs delay time and (C) pH 12.7 taken at 0.15 μs. (B and D) Simulations of A and C, respectively (radicals **5b** and **7b**). The sweep width for both spectra is 100 G.

Figure 8C the polarization of the radical from AQS is absorptive—this is a common observation in Q-band experiments, where the higher field leads to stronger radical pair mechanism (RPM)[36] polarization. The RPM is driven here by the large *g*-factor difference and has the correct phase (E for the low field radical, A for the high field signal) expected for a geminate radical pair originating from a triplet-state precursor and experiencing a negative exchange interaction. The line widths are broader here than at the X-band due to the shorter delay times of observation (uncertainty broadening).

The difference in *g*-factor between the S−S dimer structure (2.0101) and the cyclic S−N structure (2.0073) is easily understood using a resonance description. There are two main resonance structures that contribute to the stability and spin density of the cyclic cation. They have the general form $S-N^{+\bullet}$ and $^{+\bullet}S-N$. The ratio of hyperfine coupling constants in the methyl protons of the dimer to the cyclic species is 8.30/7.12 = 1.17. This tells us that the $S^{+\bullet}$ structure contributes roughly 60% to the overall *g*-factor (i.e., there is a greater spin density on the sulfur side of the three-electron bond). The remaining 40% comes from the $N^{+\bullet}$ structure, which can be estimated by considering the literature value for the *g*-factor of an alkylamine radical cation (2.0034).[37] Weighing these two *g*-factors by their appropriate percentages, we can calculate the expected *g*-factor for a $S-N^{+\bullet}$ structure: $0.6 \times (2.0101) + 0.4 \times (2.0034) = 2.0074$. This is almost exactly the observed value 2.0073. Of course, calculations of *g*-tensors from first principles are much more complicated than this, and we present the above comparison only to show that, using a fairly simple model, the correct trend can be estimated for this previously undetermined *g*-factor.

Figures 6, 7, and 8 represent solid evidence for the assignment of the TREPR signal carrier in high pH solutions of **2** with AQS to the cyclic radical cation of *N*-acetylmethionine (**7b**). Our isotopic substitutions have provided several self-consistent data sets for the existence of **7b** as a five-membered ring with the S−N three-electron bond. If the six-membered ring with a S−O three-electron bond were present instead, we would not expect an isotope effect upon substitution at the amide nitrogen, and a very different hyperfine splitting pattern would have been observed. To the best of our knowledge, this is the first room temperature liquid solution EPR characterization of any two-center three-electron bond radical cation.

A noteworthy feature of the magnetic parameters we have determined in this work is the very small hyperfine coupling for the nitrogen atom in the cyclic radical cation of *N*-acetylmethionine. This result implies that there is a very low spin density at nitrogen in this radical, which conflicts somewhat with the ab initio calculations of Huang and Rauk[19] and is a somewhat different interpretation of the field-dependent CIDNP data of Korchak et al.,[22] who studied both methionine and *N*-acetylmethionine. In the work of Champagne and co-workers,[14] the nature of the three-electron bond is described as a $\sigma-\sigma^*$ interaction and this may help explain why the coupling constant is small. If the unpaired electron is located in a σ^* orbital, it will be further away from the nucleus. Also, the remaining electrons from the lone pair on nitrogen may "shield" the unpaired electron from the nucleus.

While the calculations of Huang and Rauk may show a trend in hyperfine interactions that is physically reasonable, the fact that they were run without neighboring solvent molecules makes their absolute values somewhat suspect. The cyclic cation has a negative and positive charge, and therefore, the presence of nearby water molecules would be expected to have a large effect on its structure. In addition, if the cyclic cation is fluxional, solvent would be expected to play a large role in determining the average coupling constants. As for the field-dependent CIDNP data of Korchak et al.,[22] the authors also reported a low hyperfine coupling constant for the nitrogen and the α-carbon of *N*-acetylmethionine, which is consistent with our observations. However, they concluded from this small value for a_N that the cyclic structure was not a reactive intermediate present in *N*-acetylmethionine chemistry, or at least did not live very long. However, we have clearly shown that the *N*-acetylmethionine radical cation cannot deprotonate or form dimeric structures in basic solution, and both the *g*-factor and the proton hyperfine splittings are consistent with the cyclic species. All other candidates are ruled out by our isotopic substitution experiments and/or comparison to literature parameters.

The field-dependent CIDNP technique is not as reliable as TREPR for the determination of hyperfine couplings due to the large number of parameters needed (five in ref 22). In addition, if the cyclic and linear structures are in a dynamic equilibrium for methionine, as suggested by Goez,[21] then each method (CIDNP and TREPR) may be sampling different average values. Such averaging problems have been considered before when comparing exchange interactions in flexible biradicals using these two techniques.[38] Even a small amount of fluxional behavior in the five-membered ring may be enough to cause a considerable discrepancy between values determined by each method. Five-membered rings are notorious for such behavior and have historically been the subject of considerable discussion and debate in the field of free radical chemistry.[39]

The effects described above may be especially pronounced if the bonding interaction is weak and the bond is long. For the S−O three-electron bond, the bond length has been predicted to be 2.7 Å,[19] so this argument seems reasonable. However, we present this only as a tentative argument at the present time, as there does not appear to be any data, experimental or computational, on the length of the S−N three-electron bond in either of the two cations. Since we can rule out the S−O

SCHEME 3

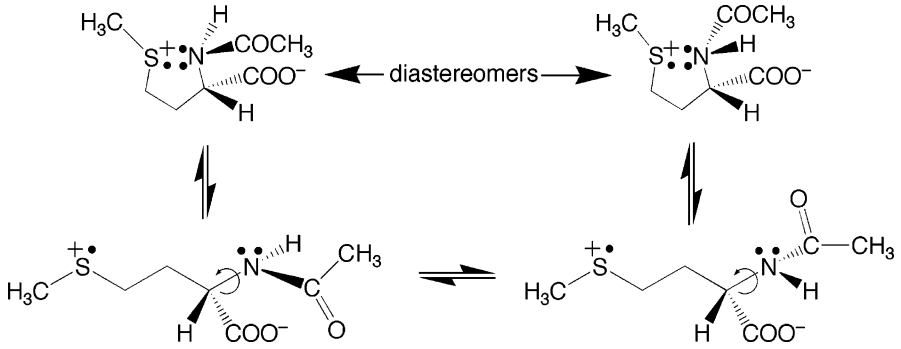

bonded structure from our isotopic substitution experiments, we conclude that the S−N bonded structure is favored, although whether it is for steric or electronic reasons is an interesting point. On the basis of the relative electronegativities, we concede that the S−O bond should be stronger. It is still possible however that the five-membered ring structure is sterically more stable because of favorable axial interactions in the ring.

It is interesting to note that a neighboring sulfur atom itself in aminyl radicals has little effect on the nitrogen hyperfine coupling. Consider the two radicals shown below:

$a_N \sim$ 10-13 Gauss (ref 30)

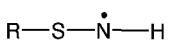

a_N = 12.3 Gauss (ref 40)

Here, the presence of an α-sulfur in the radical structure (bonded with a $\sigma-\sigma$ interaction rather than $\sigma-\sigma^*$) gives essentially the same nitrogen hyperfine coupling constant.[30,40] This suggests that the bond length and/or the $\sigma-\sigma^*$ nature of the S−N three-electron bond is more important in dictating the magnitude of the coupling constant than the identity of the neighboring atom itself.

An additional interesting feature of cation **7b** is that it can exist in two diastereomeric forms, as shown in Scheme 3. Rotation about the indicated bond allows for cyclization as long as the lone pair on the nitrogen can invert before the two-center three-electron bond can reform. Such an inversion process seems feasible and should only have a small activation barrier because we are no longer dealing with an amine but an amide. A resonance structure can be drawn by putting a double bond between the carbonyl carbon and the amide nitrogen, making its hybridization sp^2 rather sp^3. This sp^2 hybridization component will contribute to facile inversion of the lone pair.

The existence of diastereomers for radicals such as this has not previously been commented upon in the literature. It arises here because of the presence of the *N*-acetyl group and would not be observed in the methionine radical cation **7a**, which has only one stereogenic center. Of course, within a peptide sequence, this situation may be different, and thus, it should be considered whenever the N-terminus is substituted. A consequence of the diastereotopicity of **7b** is that there may exist a superposition of spectra with different hyperfine coupling constants, which may explain why the simulations are satisfactory to the naked eye but not perfect when residuals are calculated. It would certainly be expected that the two protons in the β-position to the nitrogen might have different coupling constants because the dihedral angles may be different. However, without detailed information about the rates of interconversion and pyramidalization in Scheme 3, we cannot say more about this phenomenon, and it remains a subject for further investigation.

Summary and Outlook

The radical structures for which we have provided precise magnetic parameters are shown in Table 1. Using this table and the chemistry in Schemes 1 and 2, we can summarize the work presented here as follows: Deprotonation of **1a** at any pH value to α-thio alkyl radicals **3** and **4** does not take place, and the dominant structure observed in acid solution for both starting materials (**1** and **2**) is the dimer, **5a**(**b**). In basic solution, decarboxylation to radical **8** and trapping by H_2O or HO^- to give hydroxythiyl radical **9** also appear to be slow or insignificant processes, at least on this time scale. Additionally, we see no evidence for the S−O three-electron bond leading to the six-membered cyclic radical cation **6** proposed recently for methionine amide.[16] The appearance of either the five-membered ring cation **7a**(**b**) or the neutral aminyl radical **10a**(**b**) at high pH depends only on the rate of deprotonation of the cyclic cation, which in turn depends strongly on the substitution pattern at nitrogen. Because of this substituent effect, **10a** is the only high pH radical observed for methionine oxidation, and **7b** the only paramagnetic intermediate observed when *N*-acetylmethionine is oxidized.

Future studies on these interesting structures will include labeling with ^{13}C, ^{33}S, and ^{15}N to learn more about the spin distribution in the radicals and radical cations, especially in light of the very small nitrogen hyperfine coupling constant observed in the cyclic radical cation of both methionine and *N*-acetylmethionine. The stereochemical issue raised by the diastereotopicity of radical cation **7b** is also of interest with respect to short peptides, dimers, trimers, and so forth. The memory effect observed in the aminyl radical **10a** and the resulting issue of polarization transfer from the protonated cation (Figures 2 and 3) will be modeled and presented in a future publication.

Experimental Section

All X-band (9.46 GHz) experiments were performed on a JEOL USA Inc. JES-REIX EPR spectrometer equipped with a fast preamplifier. The microwave power was 10 mW for all experiments. The aqueous solutions were circulated through a 0.4 mm quartz flat cell positioned in the center of a Varian TE_{103} optical transmission cavity. The solutions were irradiated using a Lambda Physik LPX-100i excimer laser (308 nm, XeCl) running at 60 Hz with an energy of 90 mJ (∼20 mJ hitting the sample per pulse) and a pulse width of 20 ns. All spectra were collected in the absence of field modulation at variable delay times after the laser flash using a boxcar integrator (100 ns gates), while the external magnetic field was swept over 2−4 min.

Q-band TREPR experiments (34.6 GHz) were performed using a Varian E-110 spectrometer with a modified bridge as previously described.[41] The aqueous samples were circulated

through a 0.4 mm i.d. quartz tube centered in a TE_{011} cylindrical cavity that was wire-wound to allow for sample irradiation.

All of the aqueous samples were prepared with 20 mM amino acid and 8 mM anthraquinone-2-sulfonate sodium salt (AQS) in Millipore double-distilled H_2O. The pH was adjusted with NaOH (98%, Sigma Aldrich) and measured with a Corning pH probe and meter. For experiments performed in D_2O (99.9%, Sigma Aldrich), the pD was adjusted with NaOD (99.9%, Sigma). The amino acid analogues were used as received and consisted of L-methionine (99%, Sigma), *N*-acetyl L-methionine (99%, Sigma), and *N*-acetyl L-methionine-methyl-d_3 (99%, Sigma). The AQS (97%, Sigma) was recrystallized from ethanol/H_2O before use.

Acknowledgment. This work was supported by the National Science Foundation (Grant No. CHE-0213516). A.V.Y. thanks the Russian Foundation for Basic Research (Grant No. 05-03-32370).

References and Notes

(1) Davies, M. J.; Truscott, R. J. W. *J. Photochem. Photobiol., B* **2001**, *63*, 114.

(2) Kantorow, M.; Hawse, J. R.; Cowell, T. L.; Benhamed, S.; Pizarro, G. O.; Reddy, V. N.; Hejtmancik, J. F. *Proc. Natl. Acad. Sci. U.S.A.* **2004**, *101*, 9654.

(3) (a) Butterfield, D. A.; Boyd-Kimball, D. *Biochim. Biophys. Acta* **2005**, *1703*, 149. (b) Hou, L.; Shao, H.; Zhang, Y.; Li, H.; Menon, N. K.; Neuhaus, E. B.; Brewer, J. M.; Byeon, I.-J. L.; Ray, D. G.; Vitek, M. P.; Iwashita, T.; Makula, R. A.; Przybyla, A. B.; Zagorski, M. G. *J. Am. Chem. Soc.* **2004**, *126*, 1992. (c) Clementi, M. E.; Martorana, G. E.; Pezzotti, M.; Giardina, B.; Misiti, F. *Int. J. Biochem. Cell Biol.* **2004**, *36*, 2066. (d) Misiti, F.; Martorana, G. E.; Nocca, G.; Di Stasio, E.; Giardina, B.; Clementi, M. E. *Neuroscience* **2004**, *126*, 297. (e) Butterfield, D. A.; Bush, A. I. *Neurobiol. Aging* **2004**, *25*, 563. (f) Ciccotosto, G. D.; Barnham, K. J.; Cherny, R. A.; Masters, C. L.; Bush, A. I.; Curtain, C. C.; Cappai, R.; Tew, D. *Lett. Peptide Sci.* **2003**, *10*, 413. (g) Barnham, K. J.; et al. *J. Biol.Chem.* **2003**, *278*, 42959. (h) Stadtman, E. R.; Moskovitz, J.; Levine, R. L. *Antioxid. Redox Signaling* **2003**, *5*, 577. (i) Hou, L.; Kang, I.; Marchant, R. E.; Zagorski, M. G. *J. Biol. Chem.* **2002**, *77*, 40173. (j) Kanski, J.; Aksenova, M.; Butterfield, D. A. *Neurotoxic. Res.* **2002**, *4*, 219. (k) Butterfield, D. A.; Kanski, J. *Peptides* **2002**, *23*, 1299. (l) Palmblad, M.; Westlind-Danielsson, A.; Bergquist, J. *J. Biol. Chem.* **2002**, *277*, 19506. (m) Schoeneich, C. *Arch. Biochem. Biophys.* **2002**, *397*, 370. (n) Kanski, J.; Varadarajan, S.; Aksenova, M.; Butterfield, D. A. *Biochim. Biophys. Acta* **2002**, *1586*, 190.

(4) Clancy, C. M. R.; Forbes, M. D. E. *Photochem. Photobiol.* **1999**, *69*, 16.

(5) (a) Burns, C. S.; Rochelle, L.; Forbes, M. D. E. *Org. Lett.* **2001**, *3*, 2197. (b) Morozova, O. B.; Yurkovskaya, A. V.; Tsentalovich, Y. P.; Forbes, M. D. E.; Sagdeev, R. Z. *J. Phys. Chem. B* **2002**, *106*, 1455. (c) Morozova, O. B.; Yurkovskaya, A. V.; Tsentalovich, Y. P.; Forbes, M. D. E.; Hore, P. J.; Sagdeev, R. Z. *Mol. Phys.* **2002**, *100*, 1187.

(6) Kominami S. *J. Phys. Chem.* **1972**, *76*, 1729.

(7) Kawatsura, K.; Ozawa, K.; Kominami, S.; Akasaka, K.; Hatano, H. *Radiat. Eff. Defects Solids* **1974**, *22*, 267.

(8) Naito, A.; Kominami, S.; Akasaka, K.; Hatano, H. *Chem. Phys. Lett.* **1977**, *47*, 171.

(9) Asmus, K. D.; Goebl, M.; Hiller, K. O.; Mahling, S.; Moenig, J. *J. Chem. Soc, Perkin Trans. 2* **1985**, *5*, 641.

(10) Naito, A.; Akasaka, K.; Hatano, H. *Mol. Phys.* **1981**, *44*, 427.

(11) Bobrowski, K.; Hug, G. L.; Marciniak, B.; Kozubek, H. *J. Phys. Chem.* **1994**, *98*, 537.

(12) Bobrowski, K.; Schoeneich, C.; Holcman, J.; Asmus, K. D. *J. Chem. Soc, Perkin Trans. 2* **1991**, *3*, 353.

(13) Bobrowski, K.; Schoeneich, C. *Radiat. Phys. Chem.* **1996**, *47*, 507.

(14) Champagne, M. H.; Mullins, M. W.; Colson, A. O.; Sevilla, M. D. *J. Phys. Chem.* **1991**, *95*, 6487.

(15) Tripathi, G. N. R.; Tobien, T. *J. Phys. Chem. A* **2001**, *105*, 3498.

(16) Schoeneich, C.; Pogocki, D.; Hug, G. L.; Bobrowski, K. *J. Am. Chem. Soc.* **2003**, *125*, 13700.

(17) Schoeneich, C.; Pogocki, D.; Wisniowski, P.; Hug, G. L.; Bobrowski, K. *J. Am. Chem. Soc.* **2000**, *122*, 10224.

(18) Pogocki, D.; Serdiuk, K.; Schoeneich, C. *J. Phys. Chem. A* **2003**, *107*, 7032.

(19) Huang, M.; Rauk, A. *J. Phys. Chem. A* **2004**, *108*, 6222.

(20) Goez, M.; Rozwadowski, J.; Marciniak, B. *Angew. Chem., Int. Ed.* **1998**, *37*, 628.

(21) Goez, M.; Rozwadowski, J. *J. Phys. Chem. A* **1998**, *102*, 7945.

(22) Korchak, S. E.; Ivanov, K. L.; Yurkovskaya, A. V.; Vieth, H. *Archivok* **2004**, *viii*, 121.

(23) Vuolle, M.; Makela, R. *J. Chem. Soc., Faraday Trans. 1* **1987**, *83*, 51.

(24) Muus, L. T.; Atkins P. W.; McLauchlan, K. A.; Pedersen, J. B. *Chemically Induced Magnetic Polarization*; Reidel Publishers: Dordrecht, The Netherlands, 1977.

(25) (a) Loeff, I.; Treinin, A.; Linschitz, H. *J. Phys. Chem.* **1983**, *87*, 2536. (b) Hayon, E.; Ibata, T.; Lichtin, N. N.; Simic, M. *J. Phys. Chem.* **1972**, *76*, 2072.

(26) Forbes, M. D. E. *Photochem. Photobiol.* **1997**, *65*, 73.

(27) (a) Säuberlich, J.; Brede, O.; Beckert, D. J. *J. Phys. Chem. A* **1997**, *101*, 5659. (b) Atkins, P. W.; Dobbs, A. J.; McLauchlan, K. A. *Chem. Phys. Lett.* **1973**, *22*, 209.

(28) Gilbert, B. C.; Hodgeman, D. K. C.; Norman, R. O. C. *J. Chem. Soc., Perkin Trans. 2* **1973**, *13*, 1748.

(29) Hug, G. L.; Bobrowski, K.; Kozubek, H.; Marciniak, B. *Photochem. Photobiol.* **1998**, 68, 785−796.

(30) (a) Neta, P.; Fessenden, W. *J. Phys. Chem.* **1971**, *75*, 738. (b) Tarabek, P.; Bonificac, M.; Naumov, S.; Beckert, D. *J. Phys. Chem. A* **2004**, *108*, 929. (c) Kaba, R. A.; Ingold, K. U. *J. Am. Chem. Soc.* **1976**, *98*, 7375. (d) Wardman, P.; Smith, D. R. *Can. J. Chem.* **1971**, *49*, 1869.

(31) Morozova, O. B.; Yurkovskaya, A. V.; Tsentalovich, Y. P.; Sagdeev, R. Z.; Wu, T.; Forbes, M. D. E. *J. Phys. Chem. A* **1997**, *101*, 8803−8808.

(32) (a) Morozova, O. B.; Tsentalovich, Y. P.; Yurkovskaya, A. V.; Sagdeev, R. Z. *J. Phys. Chem. A* **1998**, *102*, 3492. (b) Kaptein, R. *J. Am. Chem. Soc.* **1971**, *94*, 6202. (c) den Hollander, J. A. *Chem. Phys.* **1975**, *10*, 167. (d) Akiyama, K.; Tero-Kubota, S. *J. Phys. Chem. B* **2002**, *106*, 2398.

(33) (a) Zech, S. G.; Kurreck, J.; Renger, G.; Lubitz, W.; Bittl R. *FEBS Lett.* **1999**, *442*, 79. (b) Lakshmi, K. V.; Brudvig G. W. *Curr. Opin. Struct. Biol.* **2001**, *11*, 523. (c) Kandrashkin, Yu. E.; Vollmann, W.; Stehlik, D.; Salikhov, K.; van der Est, A. *Mol. Phys.* **2002**, *100*, 1443 and references therein.

(34) Bordwell, F. G. *Acc. Chem. Res.* **1988**, *21*, 456.

(35) Gilbert, B. C.; Trenwith, M. *J. Chem. Soc., Perkin Trans. 2* **1975**, *10*, 1083.

(36) (a) Kaptein, R. *J. Chem. Soc., Chem. Commun.* **1971**, 732. (b) Salikhov, K. M.; Molin, Y. N.; Sagdeev, R. Z.; Buchachenko, A. L. In *Spin Polarization and Magnetic Field Effects in Radical Reactions*; Molin, Yu. N., Ed.; Elsevier: Amsterdam, The Netherlands, 1984.

(37) (a) Roth, H. D.; Lamola, A. A. *J. Am. Chem. Soc.* **1975**, *97*, 6270. (b) Goez, M.; Sartorius, I. *J. Am. Chem. Soc.* **1993**, *115*, 11123.

(38) Closs, G. L.; Forbes, M. D. E.; Piotrowiak, P. *J. Am. Chem. Soc.* **1992**, *114*, 3285.

(39) Korth, H. G.; Sustmann, R.; Dupuis, J.; Groeninger, K. S.; Witzel, T.; Giese, B. *NATO ASI Series, Series C: Mathematical and Physical Sciences* **1986**, *189*, 297.

(40) Miura, Y.; Asada, H.; Kinoshita, M. *Chem. Lett.* **1978**, 1085.

(41) Forbes, M. D. E. *Rev. Sci. Instrum.* **1993**, *64*, 397.